

Changes in fibroblast morphology in response to nano-columns produced by colloidal lithography

Matthew John Dalby^{a,*}, Mathis O. Riehle^a, Duncan S. Sutherland^b, Hossein Agheli^b, Adam S.G. Curtis^a

^a Centre for Cell Engineering Institute of Biomedical and Life Sciences, University of Glasgow, Joseph Black Building, Glasgow G12 8QQ, UK

^b Department of Applied Physics, Chalmers University of Technology, Fysikgraend 3, 41296 Gothenburg, Sweden

Received 12 September 2003; accepted 19 December 2003

Abstract

In designing new biomaterials, specific chemical and topographical cues will be important in guiding cell response. Filopodia are actin-driven structures produced by cells and speculated to be involved in cell sensing of the three-dimensional environment. This report quantifies filopodia response to cylindrical nano-columns (100 nm diameter, 160 nm high) produced by colloidal lithography. Also observed were actin cytoskeleton morphology by fluorescence microscopy and filopodia morphology by electron microscopy (scanning and transmission). The results showed that the fibroblasts used produced more filopodia per μm of cell perimeter and that filopodia could often be seen to interact with the cells' nano-environment. By understanding as to which features evoke spatial reactions in cells, it may be possible to design better biomaterials.

© 2003 Elsevier Ltd. All rights reserved.

Keywords: Filopodia; Sensing; Nano-environment; Fibroblasts; Biomaterials

1. Introduction

When a tissue cell comes into contact with a biomaterial, it will perceive the chemistry of a surface using integrin transmembrane proteins in order to find suitable sites for adhesion, growth and maturation. In vitro, cells will readily translocate on the material surface to the sites of preferential attachment, and cells will produce distinct morphologies when motile and when adhered and entering the S-phase. Motile cells tend to have a rounded cell body with a leading edge (lamellipodium) and a following tail, they also tend to have small focal adhesions and many filopodia. Static cells, however, normally are well spread with many contractile stress fibres pulling the cells flat from large, established, focal adhesions (Burridge and Chrzanoska-Wodnick [1] review focal adhesions and Bershadsky et al. [2] discuss focal adhesion morphology).

As well as considering chemistry, it is becoming clear that cells must also sense their three-dimensional, topographical, environment [3]. It has been speculated that filopodia are one of the cells' main sensory tools. Gustafson and Wolpert [4] first described filopodia in living cells in 1961. They observed mesenchymal cells migrating up the interior wall of the blastocoelic cavity in sea urchins and noted that the filopodia produced appeared to explore the substrate. This led them to speculate that they were being used to gather spatial information by the cells [5]. Migrating Purkinje cells of the most caudal lobule of the cerebellar cortex of newborn rats have also been reported as probing their environment with filopodia, up to 50 μm long, presented at the cells leading edge [6].

Filopodia have been associated with the sensing of immobilised chemoattractant gradients, observed at the leading edge of cells undergoing haptotaxis [7,8]. Also linked to chemical sensing, osteoblast filopodia have been observed to anchor to synthetic hydroxyapatite (HA) islands (stoichiometrically similar to bone's natural HA) in inert composite matrices such as polyethylene (first by Huang et al. [9] and then by

*Corresponding author. Tel.: +44-141-339-885-0838; fax: +44-141-3303-730.

E-mail address: m.dalby@bio.gla.ac.uk (M.J. Dalby).

Dalby et al. [10]), polymethylmethacrylate [11] and polyethylmethacrylate [12].

With respect to topographical sensing, fibroblasts have been described as using filopodia to sense and align the cells to microgrooves [13]. Macrophages have been reported to sense grooves down to a depth of 71 nm by actively producing filopodia and elongating in response to the shallow topography [14]. More recently, fibroblast and endothelial cell filopodia have been observed to locate to random nano-islands produced by the spontaneous demixing of incompatible polymer blends [15,16]. It was, in fact, noted that as the island size was increased, the filopodia increased in thickness, until fibroblasts appeared highly stellate, with pseudopodial-like projections [15]. In a recent study, the level of stellation of the actin cytoskeleton of epithelial cells adherent on nano-structured surfaces correlated to the scale of the hemispherical nano-structures, systematically increasing from 60 nm diameter up to 170 nm diameter [16].

Once cells locate a suitable feature using the filopodia presented on the cells leading edge, lamellipodium are formed [17] which move the cell to the desired site. These actions require G-protein signalling and actin cytoskeleton. Specifically, of interest are Rho, Rac and Cdc42. Rho induces actin contractile stress fibre assembly to allow the cell to pull against the substrate, Rac induces lamellipodium formation, and Cdc42 activation is required for filopodial assembly [18]. Rho and Rac are both required for cell locomotion, but cells can translocate when Cdc42 is knocked out. Cells lacking Cdc42 cannot, however, sense chemotactic gradients and simply migrate in a random manner [19,20]. This, again, presents compelling evidence for filopodial involvement in cell sensing.

Still, however, more evidence is required to demonstrate the role of filopodia in cell-material sensing. In order to look into this, this report uses a model nano-structured biomaterial for fibroblasts to react to. Here, 160 nm high 100 nm diameter nano-columns produced by colloidal lithography were used. For this technique, an array of monodispersed nano-colloids are electrostatically assembled on a substrate and then used templated into the substrate material [21,22]. The colloids are used as an etch mask, and as the colloids are removed by the etching, so are areas of the surrounding polymer. This results in monodispersed cylindrical columns sculpted into the bulk polymer.

Cell morphology has been examined using scanning electron microscopy (SEM), transmission electron microscopy (TEM) and fluorescent microscopical observation of actin cytoskeleton. Image analysis has then been used to calculate the average number of filopodia per μm of cell perimeter on both flat control and structured materials. The combination of these results are intended to see if fibroblasts will change the number of filopodia

they produce (taking into account the changes in morphology often observed for cells cultured on topographies, and to observe if the filopodia locate to the nano-columns).

2. Materials and methods

2.1. Materials

The starting substrates for fabrication of all samples was bulk PMMA. The PMMA substrates were precut into 8 mm by 8 mm squares using a diamond saw (Loadpoint). The 1 mm thick substrates were precut to a depth of 600 μm from the backside. Colloidal lithography was used to modify the surface of the polymer producing nano-structured features. This approach is described in detail elsewhere [21–23], but in brief utilises electrostatically assembled dispersed monolayers of colloidal particles as masks for pattern transfer into substrate materials. In this work the substrate materials were pretreated with a light oxygen plasma (0.25 Torr 50w RF 120 s Batchtop) followed by electrostatic self-assembly of a multilayer of polyelectrolytes (poly(diallyldimethylammonium chloride) (PDDA, MW 200,000–350,000, Aldrich), poly(sodium 4-styrenesulphonate) (PSS, MW 70,000, Aldrich) and aluminium chloride hydroxide (ACH, Reheis)). Subsequent assembly of a colloidal mask (sulphate modified polystyrene colloid 107 ± 5 nm IDC, USA) from aqueous solution followed by drying resulted in a dispersed colloidal monolayer which has short range order, but no long range order.

The pattern of the colloidal mask was transferred into the bulk polymer using a combination of vertical and angled argon ion bombardment (250 eV, 0.2 mA/cm², 600 s at 15° from vertical followed by 840 s from vertical direction (CAIBE Ion Beam System—Oxford Ionfab)), etching was continued until the particles were completely removed resulting in cylindrical pillars. Fig. 1 shows an AFM height image of the resultant structures (tapping mode DI dimensions 3000 sharpened Silicon oxide tip NT-MDT). The height and diameter of the produced cylindrical columns are 160 and 100 nm, respectively, with a surface density of approximately $16 \mu\text{m}^{-1}$. The distribution has a short-range order and a characteristic centre-to-centre spacing (~ 230 nm) but no long-range order. The surface of the polymer is cross-linked by the argon ion etching process results in both crosslinking and removal of oxygen-rich species from the surface resulting in an altered surface chemistry compared to untreated PMMA with less surface oxygen atoms. The argon ions penetrate only relatively short distances into the polymer and modifying only a thin outer layer (5–7 nm). Flat control substrates with matched surface chemistry (characterised by XPS, data not shown here) were fabricated by subjecting flat

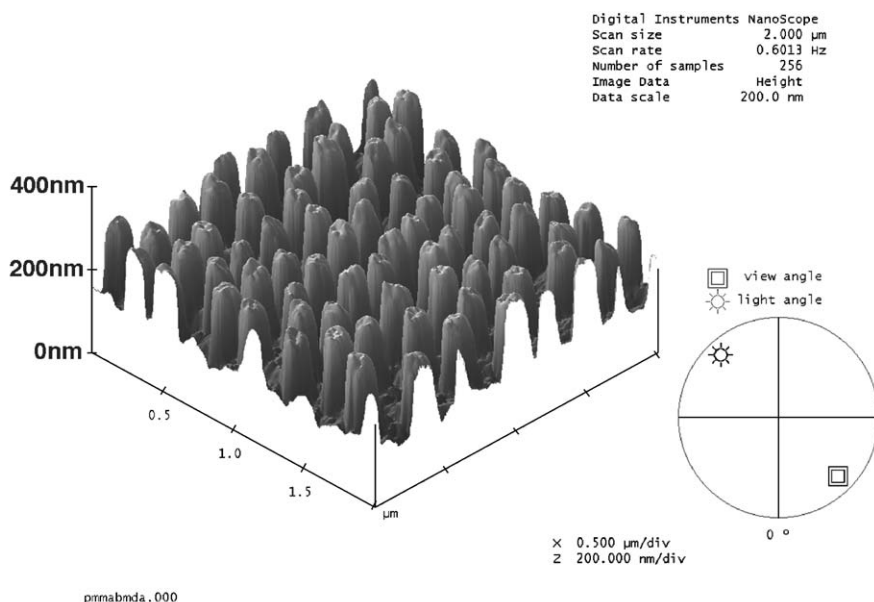


Fig. 1. Atomic force microscopical image of the 160 nm high nanocolumns.

PMMA substrates with no assembled particles to argon ion bombardment. The resultant surfaces had roughness levels around 3–5 nm (measured over 1 μm).

Samples for cell culture were snapped along the precut lines into 8 mm by 8 mm squares and blown with nitrogen to remove any particulate contamination and pre-sterilised in 70% ethanol. Fabrication and precleaning was carried out in a class 1000 clean room before packaging in airtight boxes for transfer. Finally, samples were cleaned in 70% ethanol prior to use.

2.2. Cell culture

Infinity™ telomerase immortalised human fibroblasts (hTERT-BJ1, Clonetechn Laboratories, Inc., USA) were seeded onto the test materials at a density of 1×10^4 cells per sample in 1 ml of complete medium. These cells were selected as they are genetically stable and show closer phenotypical reactions to primary cells than transformed cells, but do not undergo senescence like primary cells. The medium used was 71% Dulbeccos Modified Eagles Medium (DMEM) (Sigma, UK), 17.5% Medium 199 (Sigma, UK), 9% foetal calf serum (FCS) (Life Technologies, UK), 1.6% 200 mM L-glutamine (Life Technologies, UK) and 0.9% 100 mM sodium pyruvate (Life Technologies, UK). The cells were incubated at 37°C with a 5% CO₂ atmosphere, and the medium was changed regularly.

2.3. Image analysis of cell morphology

After 4 days of culture, the cells on the test materials were fixed in 4% formaldehyde/PBS at 37°C for 15 min. The cells were then stained for 2 min in 0.5% Coomassie

blue in a methanol/acetic acid aqueous solution, and washed with water to remove excess dye. Samples could then be observed by light microscopy and automated detection of cell outline was used to calculate individual cell length and width, perimeter, area and intensity (greyscale). The image analysis software was downloaded from the National Institute of Health (USA) (Image J, <http://rsb.info.nih.gov/ij/>). In order to calculate arboration (how much a cell deviates from being round), theoretical perimeter had to be calculated. This was done using the measured length (A) and width (B) of each cell and fitting into the formula $2\pi((A+B)/4)$. Once the theoretical perimeter was known arboration was calculated by dividing measured perimeter by theoretical perimeter. Between 50 and 60 cells were counted, and standardised illumination conditions were used throughout.

2.4. Actin observation

After 4 days of culture, the cells on the test materials were fixed in 4% formaldehyde/PBS, with 1% sucrose at 37°C for 15 min. When fixed, the samples were washed with PBS, and a permeabilising buffer (10.3 g sucrose, 0.292 g NaCl, 0.06 g MgCl₂, 0.476 g HEPES buffer, 0.5 ml Triton X, in 100 ml water, pH 7.2) added at 4°C for 5 min. The samples were then incubated at 37°C for 5 min in 1% BSA/PBS, followed by the addition of rhodamine conjugated phalloidin for 1 h at 37°C (1:100 in 1% BSA/PBS, Molecular Probes, Oregon, USA). The samples were next washed in 0.5% Tween 20/PBS (5 min \times 3) and then viewed by fluorescence microscope (Zeiss Axiovert 200M).

In order to quantify percentage cells with stress fibres, 25 cells on three replicates were counted, noting if thick stress fibres could be seen within the cell cytoplasm.

In order to quantify the numbers of filopodia, images of actin cytoskeleton were inverted and overexposed (using Adobe® Photoshop®) to allow viewing of the filopodia. Counts of filopodia for six cells on three replicates of each material were then performed and the mean and standard deviation were calculated.

2.5. Scanning electron microscopy

The cells were fixed with 1% glutaraldehyde (Sigma, UK) buffered in 0.1 M sodium cacodylate (Agar, UK) (4°C, 1 h) after a 4-day incubation period. The cells were then post-fixed in 1% osmium tetroxide (Agar, UK) and 1% tannic acid (Agar, UK) was used as a mordant, and

then dehydrated through a series of alcohol concentrations (20%, 30%, 40%, 50%, 60%, 70%, 90%, 96%, 100%). The final dehydration was in hexamethyl-disilazane (Sigma, UK), followed by air-drying. Once dry, the samples were sputter coated with gold before examination with a Hitachi S800 field emission SEM at an accelerating voltage of 10 kV.

2.6. Transmission electron microscopy

After 5 days of culture, the cells were fixed with 1.5% glutaraldehyde (Agar, UK) buffered with 0.1 M sodium cacodylate (Agar, UK) for 1 h. Cells were post-fixed with 1% osmium tetroxide, dehydrated in a series of alcohols (70%, 90%, 96% and 100%; sodium sulphate dried). Once dehydrated the samples were embedded in Spurr's resin (TAAB, UK) and polymerised at 70°C for

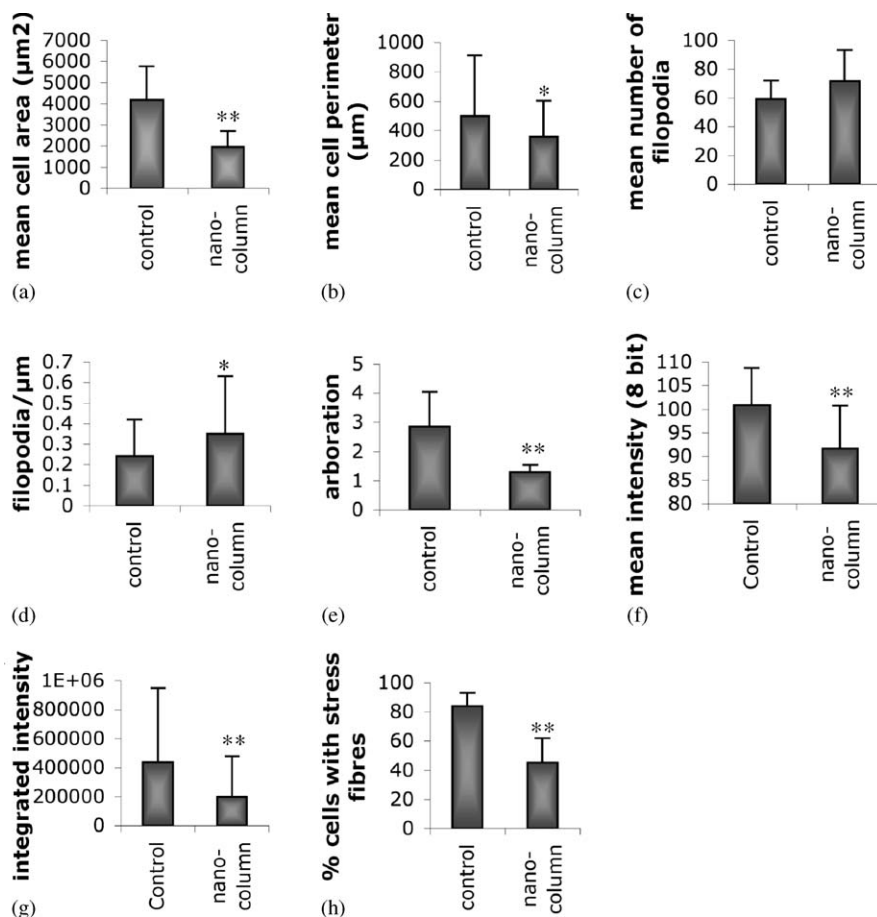


Fig. 2. Graphs quantifying cell shapes and filopodia numbers for fibroblasts cultured on flat controls and nano-columns. (a) The area of fibroblasts cultured on nano-columns was seen to be less than for cells cultured on planar control. (b) The perimeter of fibroblasts cultured on nano-columns was seen to be less than for cells cultured on planar control. (c) The mean number of filopodia produced by was seen to be similar for cells cultured on control and nano-columns. (d) The normalised number of filopodia per μm was seen to be significantly higher for cells cultured on the nano-columns compared to planar control. (e) Mean arboration (measured perimeter/theoretical perimeter) was seen to be reduced for cells on the nano-columns compared to those on control, showing that the cells were more rounded on the nano-columns. (f) The intensity (greyscale measurement) was seen to decrease for cells cultured on the nano-columns. (g) The integrated intensity (intensity \times area) was seen to be decreased for fibroblasts grown on the nano-columns compared to those on the planar controls. (h) The percentage population of cells with clearly defined stress fibres was seen to decrease when cultured on the nano-columns compared to flat control. Results are the mean \pm sd; * = *t*-test, $p < 0.05$; ** = *t*-test, $p < 0.01$.

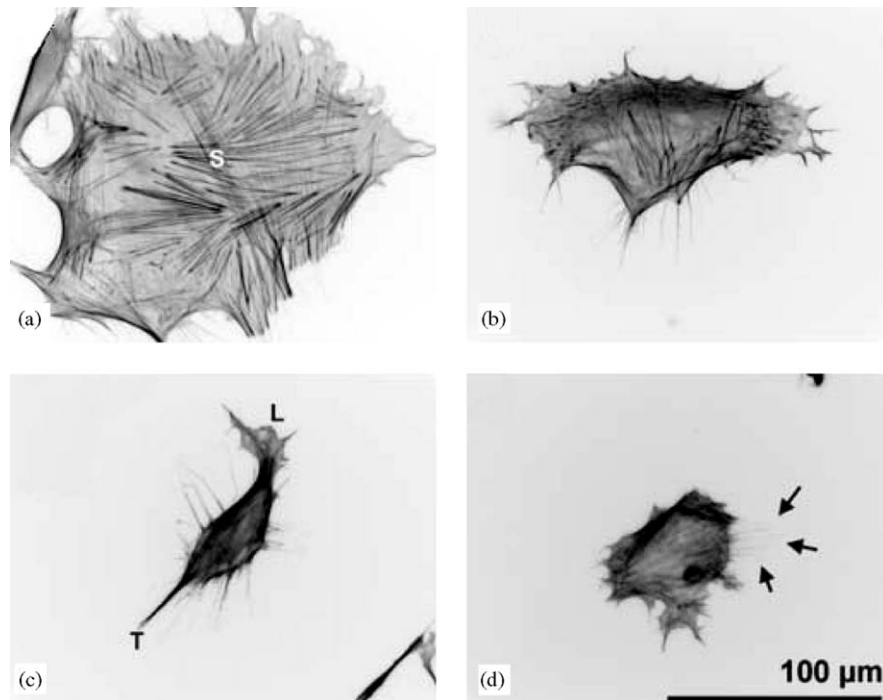


Fig. 3. Fluorescent actin staining (images inverted to show filopodia more clearly). (a and b) Fibroblasts on control, (c and d) fibroblasts on nano-columns. (a) A well spread cell with many stress fibres (s); (b) cells becoming well spread, but still with a polarised morphology; (c) a rounded cell that is clearly polarised with lamellipodia at the leading edge (L) and a trailing tail (T); (d) spreading cell, which is still notably smaller, and has fewer stress fibres than the cells seen in (a and b) (arrows point to faint filopodia).

18 h. Ultrathin sections were cut, stained with uranyl acetate (2% aq) and lead citrate, and viewed with a Zeiss TEM.

2.7. Statistics

Throughout, student's *t*-test (for two samples, assuming unequal variances) was used to compare statistical significance of test materials against the control. Results of $p < 0.05$ were considered significant (differences $p < 0.05$ denoted by *, $p < 0.01$ denoted by **).

3. Results

Calculation of the mean number of filopodia per fibroblast showed that there was a small (non-significant) increase in the number of filopodia per cell for h-TERT's cultured on the structured material or the flat control (Fig. 2c). Quantification of cell area and perimeter length showed that cells cultured on the nano-columns had a significantly smaller areas and perimeters than for cells cultured on flat controls (Fig. 2a and b). By dividing the number of filopodia by the cell perimeters, numbers of filopodia per μm could be calculated, and this result showed that the cells on the nano-columns produced significantly more filopodia

per μm of membrane than cells on the planar controls (Fig. 2d).

Aboration (measured perimeter/theoretical perimeter) gives a measure of how round the main cell body is (image analysis was not sensitive enough to include filopodia), with the intention being that the less well spread a cell is, the more round it will be. The results shown in Fig. 2e represent the overall shape of the cells (since filopodia are not included). The cells on the nano-columns had less arboration than those on the flat controls. In order to further examine cell spreading on the substrates, images of Coomassie blue stained cells (the amount of Coomassie blue bound is a measure of the amount of protein present, thus thicker layers absorb more light) were studied. The mean intensity, a measure of cell thickness, was lower for the cells on the nano-columns (Fig. 2f). The integrated intensity (intensity multiplied by area) gives an approximation of total cell protein (as Coomassie blue labels protein), and the results showed that the cells on the nano-columns contained less protein than those on the flat materials, which equates to the cells having smaller volumes (Fig. 2g). These results show that the cells were smaller, thicker and more rounded when grown on the nano-columns than when cultured on the planar controls.

In order to quantify actin organisation, percentage of cells on the substrates with thick stress fibres (contractile in appearance (labelled 's' in Fig. 3a)) through the

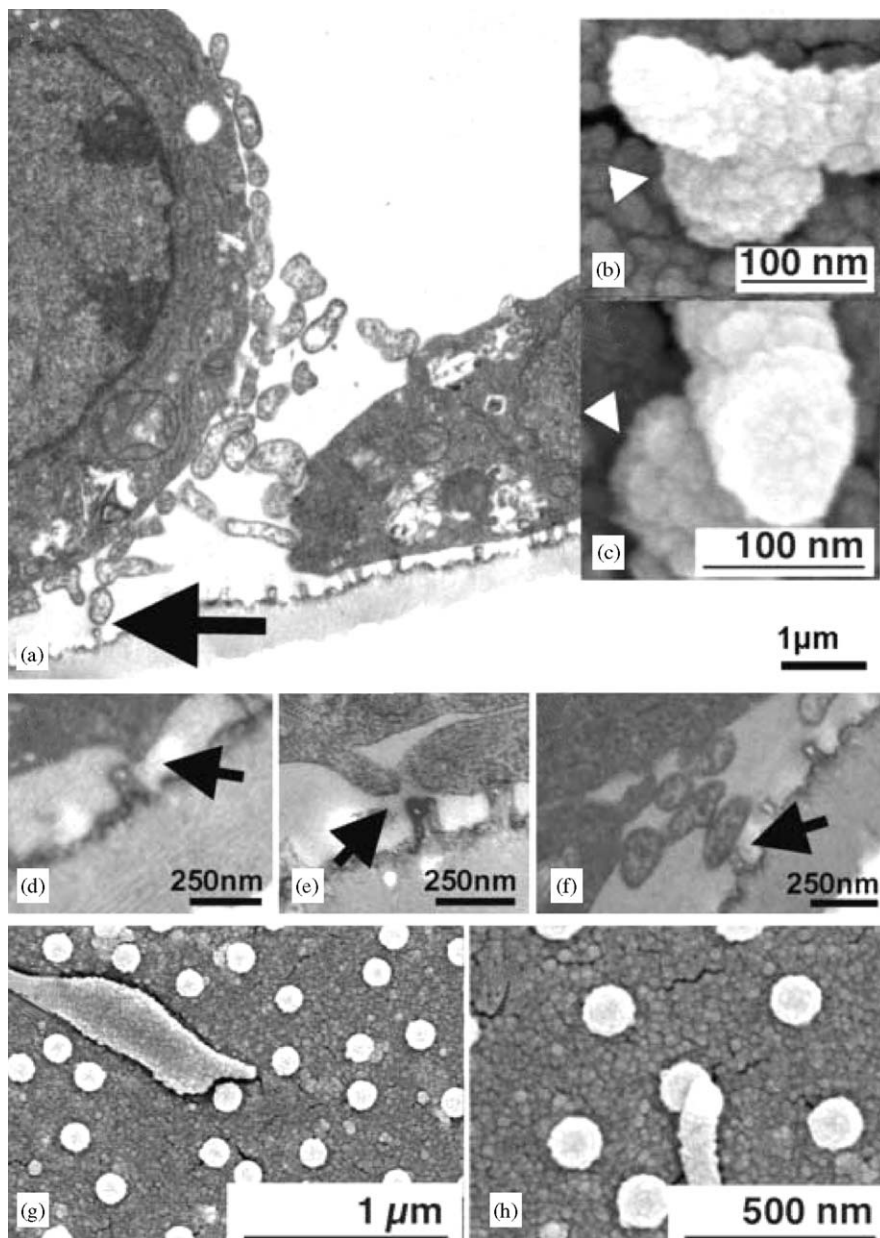


Fig. 4. Electron micrographs of filopodia reacting to nano-columns. (a) TEM section of a rounded cell with many filopodia, arrow shows filopodia/nano-column interaction. (b and c) High magnification SEM's of filopodia bending upon contacting nanocolumns (nano-columns shown by arrowhead). (d–f) More TEM's of filopodia/nano-column interactions (arrows show interactions). (g and h) Low magnification SEM's of filopodia/nano-column interactions.

cytoplasm were calculated. A significantly higher population of cells containing these non-peripheral stress fibres was noted on the flat control compared to the nano-columns (Fig. 2h).

Observation of actin clearly showed different cell morphologies for cells on the nano-columns compared to control (Fig. 3). As indicated by the quantification of cell perimeter (Fig. 2a), the cells were well spread, with many stress fibres apparent, on the controls (Fig. 3a and b). Fig 3(a) shows a notably well spread cell, whilst Fig. 3(b) shows a cell changing from polarised to flattened morphology, with stress fibres developing in the lamellae

region. Cells on the nano-columns, however, were less well spread (Fig. 3c and d). Many were highly polarised with areas of dense filopodia extension (Fig. 3c), some cells were flattening on the nano-columns, but with reduced size, and less apparent stress fibre formation, compared to cells on the planar controls (Fig. 3d).

Electron microscopy (both scanning and transmission) was used to look for specific filopodial/nano-column interaction, and this was regularly observed (Fig. 4). TEM was used to observe underneath the cells, whilst SEM was used to look to the side of the cells, regular interaction was observed with both;

for cell underside see Fig. 4a, d–f, for extensions to the side of the cells see Fig. 4b and c (high magnification) and g and h (low magnification). In SEM images, the shape of individual filopodia could be determined and the filopodia often appeared to have deformed when encountering a nano-column, usually by bending (Fig. 4b,c,g and h).

4. Discussion

The results in this study show that the cell perimeter for cells cultured on the nano-columns was reduced compared to fibroblasts grown on flat control. Results for area, arborisation and intensity agreed with the perimeter measurements, and also showed that the cells had a more rounded cell body. It is noted that whilst the standard deviations were high, that this is to be expected due to biological variation and stage of cell cycle, and that sufficient cell numbers had to be analysed to generate data from which trends could be derived.

The results in this study also showed that the number of filopodia were slightly increased (by 17%) in fibroblasts cultured on the nano-columns compared to control; however, once the results were normalised to produce filopodia per μm , it was shown that the number of filopodia per μm was then significantly greater for cells cultured on the nano-columns (by 31%). This result is in agreement with the measurement of cell periphery and area, again showing that the cells were more rounded when cultured on the nano-columns. In addition, electron microscopical study showed regular filopodia/nano-column interaction.

Anchorage dependent cells, such as fibroblasts, need to spread in order to enter G1 and G2 of the cell cycle [24]. Cells use contractile actin stress fibres to spread on to material surfaces, and it has been shown in this study that whilst cells on the planar controls have many stress fibres, and hence are flat, cells on the nano-columns have fewer stress fibres, and are thus less spread and more rounded. Rather, cells on the nano-columns had more regular expression of filopodia. Filopodia are driven by actin acting upon the plasma membrane, and actin is observed in filopodia as tight parallel bundles (the thicker stress fibres are only seen once the filopodia are attached) [1].

Thus, it appears that rather than adhering and spreading (as is apparent in cells on the planar controls), fibroblasts on the nano-columns were rather more polarised with rounded cell bodies having a higher density of filopodia, with the filopodia probing the nano-structured environment surrounding the cell (shown by electron microscopy). It is noted that filopodia are highly motile structures, sweeping from side to side at the cells leading edge (and elsewhere), thus it could be suggested that these images are purely chance observations. However, the observation of filopodia

bending in response to these structures suggests that they are locating areas of ‘interest’, even though the chemistry across the surface was homogeneous.

5. Conclusions

The nano-columns used in this study were around 160 nm high, 100 nm wide, and whilst small in comparison the main cell body, they appear to be easily detected by the fine, approximately 50–70 nm wide, filopodia. These results add to the theory that filopodia are involved in gathering special information from the cells environment.

When designing new-generation tissue engineering materials, it will be important to present cells with cues that will effect responses. The desired response may be to align the cells, to increase motility, to increase or reduce proliferation and to alter differentiation. In all these cases, the cells will have to sense their environment (both chemically and topographically), and it appears that filopodia are important in this process—perhaps acting as ‘cats whiskers’. It is now necessary to calculate the range and scale of features that cells can sense, and to evaluate the range of responses generated.

Acknowledgements

Matthew Dalby is a BBSRC David Phillips Fellow (17/JF/20604). This work was also supported by the EU framework V grant QLK3-CT-2000-01500 (Nanomed). We would like to thank Mrs Margaret Mullin and Mr Ioin Robertson of the Glasgow University Integrated Microscopy Facility for help with EM preparation. We also thank Prof Chris Wilkinson for his interesting discussion and Mr Andy Hart, Mr Gregor Aitchison and Mrs Allison Beattie for technical help.

References

- [1] Burridge K, Chrzanowska-Wodnick M. Focal adhesions, contractility, and signaling. *Annu Rev Cell Dev Biol* 1996;12: 463–519.
- [2] Bershadsky AD, Tint IS, Neyfakh Jr AA, Vasiliev JM. Focal contacts of normal and RSV-transformed quail cells. Hypothesis of the transformation-induced deficient maturation of focal contacts. *Exp Cell Res* 1985;158:433–44.
- [3] Curtis ASG, Wilkinson CDW. Nanotechniques and approaches in biotechnology. *Trends Biotechnol* 2001;19:97–101.
- [4] Gustafson T, Wolpert L. Studies on the cellular basis of morphogenesis in the Sea Urchin embryo: directed movements of primary mesenchyme cells in normal and vegetated larvae. *Exp Cell Res* 1961;24:64–79.
- [5] Wood W, Martin P. Structures in focus—filopodia. *Int J Biochem Cell Biol* 2002;34:726–30.

- [6] Morris RJ, Beech JN, Barber PC, Raisman G. Early stages of Purkinje cell maturation demonstrated by Thy-1 immunohistochemistry on postnatal rat cerebellum. *J Neurocytol* 1985;14:427–52.
- [7] Ueda M, Sako Y, Tanaka T, Devreotes P, Yanagida T. Single-molecule analysis of chemotactic signalling in dictyostelium cells. *Science* 2001;294:864–7.
- [8] Iijima M, Devreotes P. Tumor suppressor PTEN mediates sensing of chemoattractant gradients. *Cell* 2002;109:599–610.
- [9] Huang J, Wang M, Tanner KE, Bonfield W, Di Silvio L. In vitro mechanical and biological assessment of hydroxyapatite reinforced polyethylene composite. *J Mater Sci: Mater Med* 1997;8:775–9.
- [10] Dalby MJ, Di Silvio L, Gurav N, Annaz B, Kayser MV, Bonfield W. Optimizing HAPEX™ topography influences osteoblast response. *Tissue Eng* 2002;8:453–67.
- [11] Dalby MJ, Di Silvio L, Harper EJ, Bonfield W. Increasing hydroxyapatite incorporation into poly(methylmethacrylate) cement increases osteoblast adhesion and response. *Biomaterials* 2002;23:569–76.
- [12] Opara TN, Dalby MJ, Harper EJ, Di Silvio L, Bonfield W. The effect of varying hydroxyapatite in poly(ethylmethacrylate) bone cement on human osteoblast-like cells. *J Mater Sci: Mater Med* 2003;14:277–82.
- [13] Clark P, Connolly P, Curtis ASG, Dow JAT, Wilkinson CDW. Topographical control of cell behaviour: II. Multiple grooved substrata. *Development* 1990;108:635–44.
- [14] Wojciak-Stothard B, Curtis A, Monaghan W, MacDonald K, Wilkinson C. Guidance and activation of murine macrophages by nanometric scale topography. *Exp Cell Res* 1996;223:426–35.
- [15] Dalby MJ, Riehle M, Johnstone HJH, Affrossman S, Curtis ASG. Polymer demixed nano-topography: control of fibroblast spreading and proliferation. *Tissue Eng* 2002;8:1099–108.
- [16] Dalby MJ, Riehle M, Johnstone HJH, Affrossman S, Curtis ASG. In vitro reaction of endothelial cells to polymer demixed nano-topography. *Biomaterials* 2002;23:2945–54.
- [17] Andersson A-S, Olsson P, Lidberg U, Sutherland DS. Influence of nanoscale topography on the morphology of two epithelial cell types. *IEEE Trans Nanobiosci* 2003;2:49–57.
- [18] Schmitz AA, Govek EE, Bottner B, Van Aelst L. Rho GTPases: signalling, migration, and invasion. *Exp Cell Res* 2002;261:1–12.
- [19] Jones GE, Allen WE, Ridley AJ. The rho GTPases in macrophage motility and chemotaxis. *Cell Adhes Commun* 1998;6:237–45.
- [20] Ridley AJ, Allen WE, Peppelenbosch M, Jones GE. Rho family proteins and cell migration. *Biochem Soc Symp* 1999;65:111–23.
- [21] Hanarp P, Sutherland DS, Gold J, Kasemo B. Control of nanoparticle film structure for colloidal lithography. *Colloids Surf* 2003;A214:23–36.
- [22] Denis FA, Hanarp P, Sutherland PS, Dufrène YF. Fabrication of nanostructured polymer surfaces using colloidal lithography and spin-coating. *Nanoletters* 2002;2:1419–25.
- [23] Hanarp P, Sutherland D, Gold J, Kasemo B. Nanostructured model biomaterial surfaces prepared by colloidal lithography. *Nanostruct Mater* 1999;12:429–32.
- [24] Folkman J, Moscona A. Role of cell shape in growth control. *Nature* 1978;273:345–9.